

A composite study of the MJO influence on the surface air temperature and precipitation over the Continental United States

Shuntai Zhou · Michelle L’Heureux ·
Scott Weaver · Arun Kumar

Received: 3 November 2010 / Accepted: 17 January 2011 / Published online: 1 February 2011
© Springer-Verlag 2011

Abstract The influence of the MJO on the continental United States (CONUS) surface air temperature (SAT) and precipitation is examined based on 30 years of daily data from 1979–2008. Composites are constructed for each of the eight phases of the Wheeler-Hendon MJO index over 12 overlapping three-month seasons. To ensure that the MJO signal is distinguished from other patterns of climate variability, several steps are taken: (a) only days classified as “MJO events” are used in the composites, (b) statistical significance of associated composites is assessed using a Monte Carlo procedure, and (c) intraseasonal frequencies are matched to the unfiltered data. Composites of other fields are also shown in order to examine how the SAT and precipitation anomalies are associated with large-scale circulations providing a link between the tropics and extratropics. The strongest and most significant MJO effects on SAT are found during the northern winter seasons. When enhanced convection is located over the equatorial Indian Ocean, below-average SAT tends to occur in New England and the Great Lakes region. As enhanced tropical convection shifts over the Maritime continent, above-average SAT appears in the eastern states of the US from Maine to Florida. The MJO influence on precipitation is also significant during northern winter seasons. When enhanced convection is located over the Maritime continent, more precipitation is observed in the central plains of the US. Enhanced precipitation also occurs over the west coast of the US when convective activity is

stronger over the Indian Ocean. During the northern summer and fall, the MJO impact on precipitation is mainly significant at lower latitudes, over Mexico and southeastern US.

1 Introduction

The Madden-Julian Oscillation (MJO) is the most important atmospheric mode of intraseasonal variability in the tropics, characterized by a 30–60 day atmospheric oscillation propagating eastward along the equator (Madden and Julian 1994; Knutson and Weickmann 1987). The MJO has a large impact on tropical weather, such as the Indian, Australian and North American summer monsoons and the formation and strength of hurricanes and tropical storms (Hendon and Liebmann 1990; Maloney and Hartmann 2000a, b; Hall et al. 2001; Lorenz and Hartmann 2006; Donald et al. 2006; Pai et al. 2009; Klotzbach 2010).

It has been noted in previous studies that the MJO can interact with extratropical circulations through modulating the East-Asian jet stream and convectively forced Rossby wave dispersion (Lau and Phillips 1986; Chang and Lim 1988; Higgins and Mo 1997; Straus and Lindzen 2000; Matthews 2006). The forcing arising from the modulation of tropical convection is likely behind the relationship of the MJO with other extratropical climate modes, such as the Pacific and North American mode (PNA), the Arctic Oscillation (AO) and the North Atlantic Oscillation (NAO) (Zhou and Miller 2005; L’Heureux and Higgins 2008; Mori and Watanabe 2008; Lin et al. 2009). Therefore, the MJO has an impact on the weather and climate over North America. For instance, more extreme precipitation in California is related to the MJO during the northern winter (Jones 2000). Large MJO effects on precipitation in the states of Oregon and Washington were observed in both the

S. Zhou (✉) · M. L’Heureux · S. Weaver · A. Kumar
NOAA/NWS/NCEP, Camp Springs, MD 20746, USA
e-mail: shuntai.zhou@noaa.gov

S. Zhou
Wyle, Inc., McLean, VA 22102, USA

early and late winter (Bond and Veehi 2003). Similar connections between the MJO and surface air temperature (SAT) were found in Canada during wintertime (Lin and Brunet 2009).

Due to the broad tropical and extratropical impacts of the MJO on intraseasonal timescales, better understanding of the MJO could potentially improve extended range forecasts of week-two and beyond, particularly when there is an on-going MJO event. Numerical and empirical model experiments have shown the potential predictability of the MJO out to 3 weeks (Jones et al. 2000; Waliser et al. 2003; Lo and Hendon 2000). In this study, our objective is to develop composites to provide a comprehensive, large-scale overview of the MJO impact on the SAT and precipitation over the continental United States (CONUS) across all seasons. We also present the quantitative estimate of the potential predictability from the use of MJO composites. In the next section, a brief description of the data and the MJO index is given. In Sect. 3 we explain the composite methodology and procedures. The composite results for SAT and precipitation are discussed in Sects. 4 and 5, respectively. The forecast skill from the use of composites is estimated in Sect. 6. A conclusion is given in Sect. 7.

2 Data and the MJO index

We use 30 years (1979–2008) of daily data of SAT and precipitation for CONUS and the US-Mexico area to make composites according to different MJO phases. Daily CONUS SAT data are obtained from the NCDC Cooperative station data and are gridded to $1^\circ\text{lat} \times 1^\circ\text{lon}$ grid (Janowiak et al. 1999). Daily precipitation data are obtained from the real-time $0.25^\circ\text{lat} \times 0.25^\circ\text{lon}$ gridded precipitation dataset of Higgins et al. (2000). Because the time series of daily precipitation data is intermittent and has large variations, we apply a five-day running average to reduce the noise prior to composite analysis. The so-called “raw data” anomalies are calculated by removing the annual cycle and linear secular trend.

While there are various MJO indices found in the literature, the Wheeler-Hendon (WH) MJO Index has been commonly used for the MJO monitoring and prediction (Wheeler and Hendon 2004). The WH MJO Index is a combination of two leading PCs of multivariate empirical orthogonal function (EOF) analysis (commonly referred to as RMM1 and RMM2), which is based on the combined fields of outgoing longwave radiation (OLR), 850 and 200-hPa zonal wind anomalies. It is naturally divided into eight phases in the two-dimensional space formed by the two PCs (also called the Wheeler-Hendon diagram). Each phase corresponds to a particular stage of the MJO life cycle. For instance, Phases 2 and 3 are associated with

enhanced convection over the Indian Ocean, while Phases 4 and 5 denote convection centers over the Maritime continent, as shown in Fig. 1. The amplitude of the MJO index, or the radius in the WH diagram, indicates the strength of MJO events. When a time series of MJO index is plotted in the Wheeler-Hendon diagram, counterclockwise movement represents eastward propagation.

In this study we use the WH MJO Index as the basis for the composites of SAT and precipitation. Because there is a WH MJO index value each day, whether there is an MJO event or not, the data are subjectively analyzed to identify “MJO event days.” An MJO event is identified by periods that generally have amplitude greater than one and demonstrate eastward propagation. Further, to be categorized as an MJO event, the event must last longer than 25 days and not remain stationary for 20 days or more.

3 Composite methodology

Since the raw data of SAT and precipitation contain all temporal frequencies, the composite may not truly represent MJO or intraseasonal frequencies. Although we could use a band-pass filter to remove unwanted signals, real-time prediction involves an unknown future state and requires the prediction of unfiltered data. Therefore, to ensure that composites are associated with the MJO, we take three steps in the composite analysis. This procedure is illustrated in Fig. 2. First, we only use days classified as MJO events. Secondly, we test the statistical significance of the composites using a Monte Carlo procedure. The final step is the “intraseasonal match”, in which we compare time series of the raw data and the 20–100 day band-pass

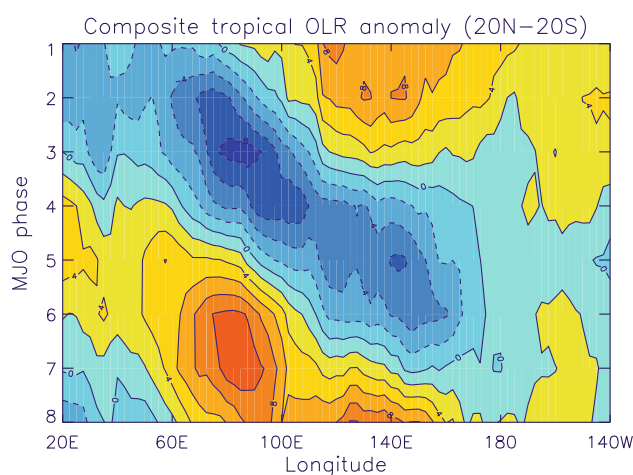


Fig. 1 Composite of tropical outgoing longwave radiation (OLR) anomalies (W m^{-2}) between 20°E and 140°W (averaged between 20°N and 20°S). The composite is based on all seasons and 21 years of pentad OLR data (1979–1999). Blue shadings (negative values) indicate cloudiness and convective activity

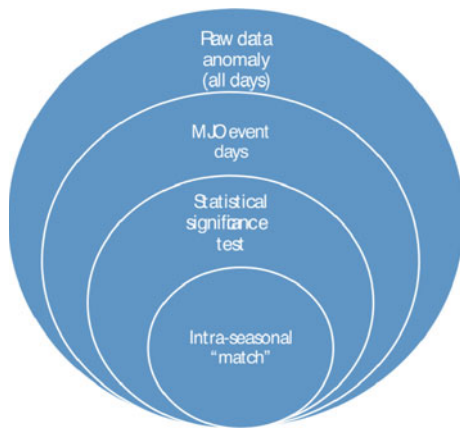


Fig. 2 Schematic of the composite methodology from the raw data (*outer region*) to the more stringent intraseasonal “matching” procedure (*inner region*)

filtered data to determine the extent that the sign of the anomalies match each other (e.g., both datasets indicate above average temperatures). This way, in real-time, a forecaster can select how much agreement is desired between the raw data anomalies and the expected anomalies on intraseasonal timescales.

Over the 30-year period, MJO events are identified approximately 54% of the time. The number of MJO days is seasonally dependent, as listed in Table 1. There are fewer MJO days identified in the northern summer (JJA) compared to other seasons. The number of MJO events also varies from year to year. In this study, all composites are made on a seasonal basis in order to take into account seasonal differences. The composites of US temperature and precipitation are contemporaneous with the eight MJO phases, so lead-lag relationships are not explicitly considered. Therefore, the US impacts associated with an MJO phase may be forced by tropical anomalies based on previous MJO phases due to the time lag between the tropics and extratropics (Jin and Hoskins 1995).

We use the Monte Carlo method (sampling with replacement) to test the statistical significance of the MJO

composites. Specifically, a large number (800) of random composites are made for each season, using the historical record of SAT and precipitation. In these random composites, the degrees of freedom are kept the same as the MJO composites. In the observations, as the MJO spends several days within the same phase, the adjacent days are autocorrelated lowering the effective degrees of freedom of each composite. To take this into account, if the observations include N consecutive days within the same MJO phase, then N days are also selected for the random sample. Figure 3 (right panel) shows an example of the resulting statistical significance percentages of SAT composites for December-February (DJF). The percentages indicate the percent chance that the anomalies arise from random chance. Figure 3 (left panel) also shows the unmasked composite based on the raw anomalies. Showing the anomalies next to the significance map enables forecasters to select how much random chance they are willing to tolerate.

To estimate the degree that the composite anomalies are due to intraseasonal or MJO timescales, we match the time series of the raw data with the 20–100 day band-pass filtered data (Murakami 1979). The peak of remaining signal in the filtered data is a 45-day period, a typical MJO life cycle. Both the raw data and filtered data are normalized by their own standard deviations of daily variability. To define days with “intraseasonal match”, “above-average” and “below-average” anomalies for the filtered and unfiltered time-series are defined by plus or minus one standard deviation. The percentage of match, which varies from 0 to 100%, indicates the percent of days that are in agreement between the raw, unfiltered anomalies and filtered MJO frequencies, and further, are greater than one standard deviation.

4 Composites of surface air temperature

The composites of SAT in CONUS are created for twelve overlapping three-month seasons (i.e. DJF, JFM, FMA,

Table 1 Numbers of MJO days in the 1979–2008 (30 years) period

	DJF	JFM	FMA	MAM	AMJ	MJJ	JJA	JAS	ASO	SON	OND	NDJ
Phase 1	131	187	191	236	200	226	211	109	200	196	173	147
Phase 2	164	192	177	208	185	167	173	207	247	251	207	200
Phase 3	218	213	183	203	165	134	97	99	131	188	224	253
Phase 4	188	191	224	202	185	121	88	95	150	197	204	180
Phase 5	166	161	158	181	163	116	131	172	240	231	213	184
Phase 6	199	196	201	207	195	165	139	126	173	195	205	193
Phase 7	236	214	232	243	205	182	115	103	110	145	208	215
Phase 8	180	211	206	255	211	190	133	134	143	158	167	187

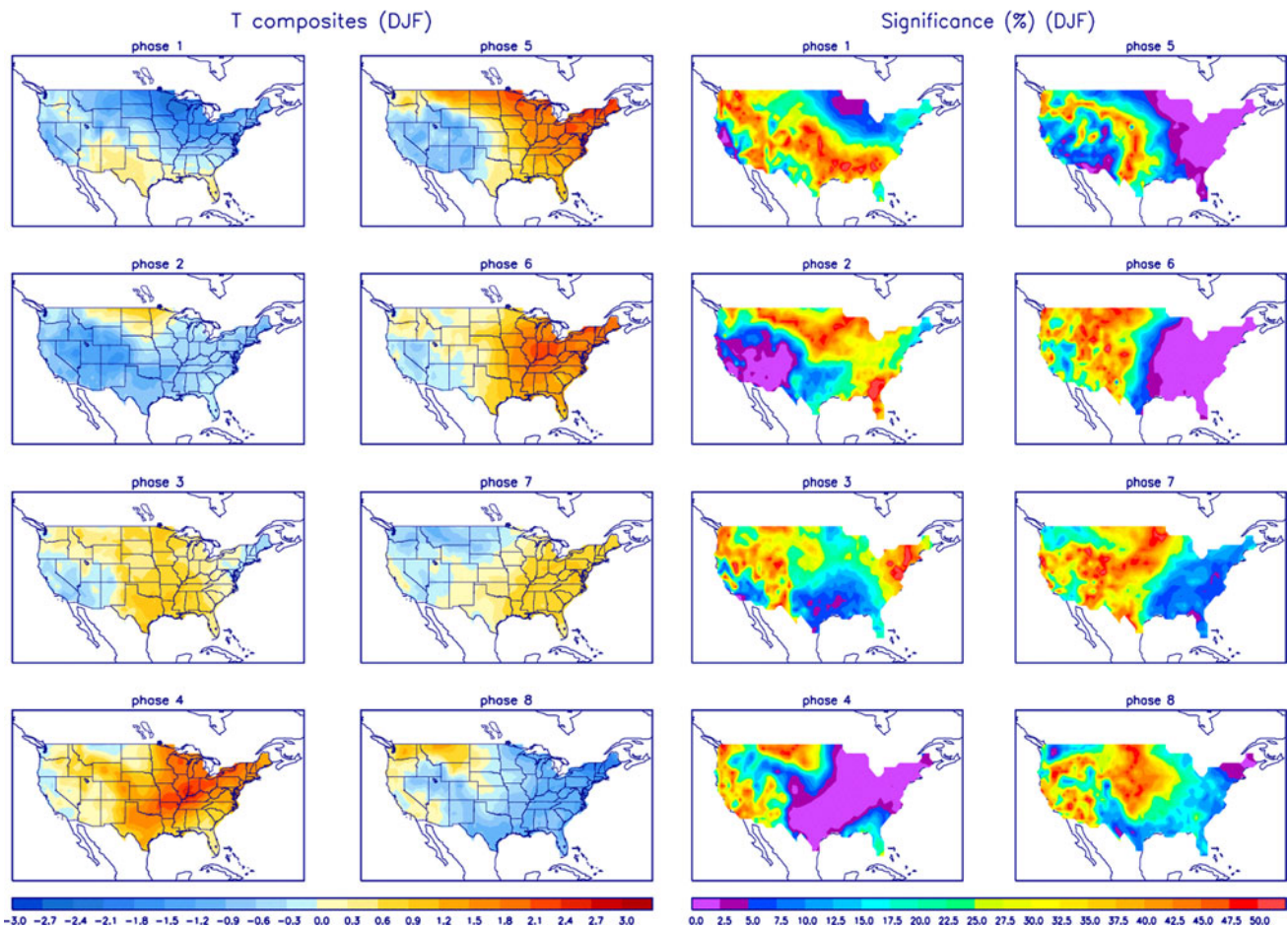


Fig. 3 (left 8 panels) December–February (DJF) composites of surface air temperature anomalies ($^{\circ}\text{C}$) for each of the eight MJO phases. (right 8 panels) The statistical significance of the DJF surface air temperature composites shown in the left panels. The percentage indicates the chance that the temperature anomalies shown the left

panels arise from random chance (using a Monte Carlo procedure with replacement). Purple/blue areas represent regions of higher confidence (and therefore a lower percent chance that the anomalies are random)

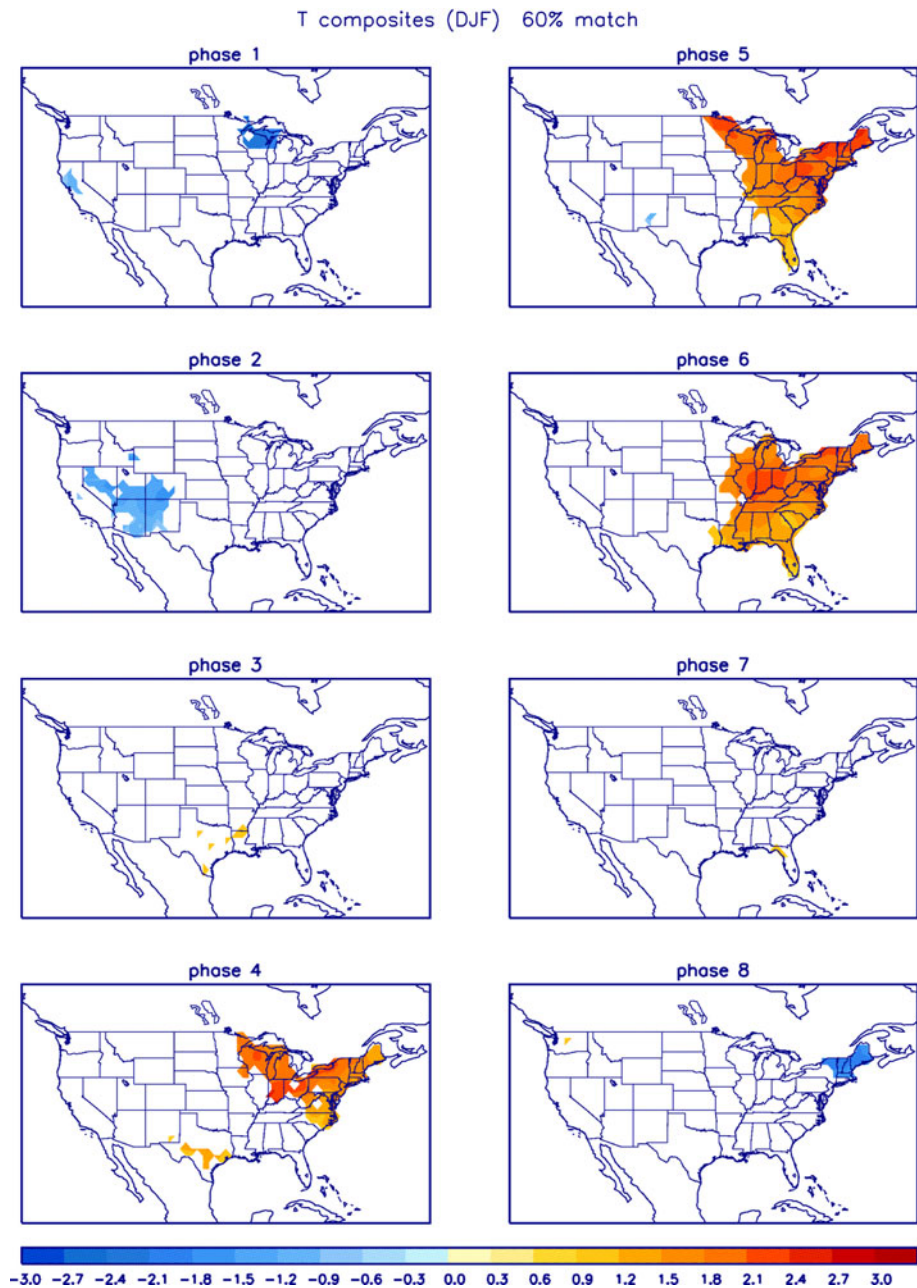
etc.). Figure 4 shows the DJF composites of SAT in each MJO phase, where shaded areas are 95% statistically significant based on the Monte Carlo test and a 60% threshold is selected for the intraseasonal match. During the northern winter season there are strong MJO signals in the SAT anomalies. Large above-average anomalies are found in MJO phases 4, 5 and 6 across eastern portion of the CONUS from Maine to Florida. Lin and Brunet (2009) showed the above-average SAT anomalies also extend into eastern Canada, particularly in MJO phases 4 and 5. Significant below-average SAT anomalies are seen in MJO phases 8 and 1 in New England and the Great Lakes region, but the area is much smaller than the above-average anomalies. However, as shown by Fig. 3, larger regions of below-average SAT anomalies are evident if a lower statistical significance threshold is chosen (e.g. $<10\%$).

To verify that the significant SAT anomalies in the eastern US are MJO related, we do a point check by examining an SAT time series. Figures 5a and b display RMM1 and

RMM2 values for warm and cold days separately for all days which are in the MJO composites of the 30 DJF seasons, respectively, for the chosen point near New York (42°N , 75°W). Figures 5c and d show the frequency of warm and cold days as a function of the MJO phase. Here the SAT anomaly is based on the band-pass (20–100 day) filtered data in order to emphasize intraseasonal variability. The SAT anomalies have a clear preference according to the MJO phase. There is a notable shift from above-average anomalies (in phases 4, 5 and 6) to below-average anomalies (in phases 8, 1, and 2). We also plotted the SAT anomalies with the raw data and, although showing more scatter, there is clear evidence of similar MJO phasing (not shown).

The composites for all other seasons can be found on the NOAA Climate Prediction Center (CPC) website: (<http://www.cpc.ncep.noaa.gov/products/precip/CWlink/MJO/Composites/Temperature/>). Other than northern winter seasons (NDJ, DJF, JFM) the MJO influence on SAT is generally small. Except for some small signals in a

Fig. 4 Composites of December–February surface air temperature anomalies ($^{\circ}\text{C}$) as a function of the 8 MJO phases. The composites are based on 30 years (1979–2008) of daily data. The *white* area represents areas where the percentage of random chance is greater than 5% or less than the 95% confidence level (see *right* panels in Fig. 3) and an intraseasonal match less than 60%



couple MJO phases, the MJO signal is quite weak and negligible during much of the year. Figure 6 shows the percentages of the SAT composite areas which are statistically significant at 95% confidence and with different intraseasonal match levels. During the northern winter seasons, the area with 60% intraseasonal match covers about 30–40% of CONUS in MJO phases 5 and 6, while during other seasons, the area is mostly less than 10%. One may ask why the MJO effect on the SAT is strong only during the northern winter and for MJO phases 4, 5 and 6. We speculate that winter SAT in North America is largely influenced by shifts in the East Asian jet stream and associated Rossby wavetrains, which are stronger during

the winter months (e.g. Lau and Phillips 1986; Lin and Brunet 2009). It is possible that the large warm SAT anomaly during MJO phases 4, 5 and 6 can be traced to the tropical forcing of MJO phases 2 and 3, considering that it takes approximately 2 weeks for tropical MJO waves to propagate to North America. Lin et al. (2010) also showed that when convection is active over the Indian Ocean (MJO phases 2 and 3) the MJO is more effective in forcing extratropical circulation anomalies. During other seasons, the MJO signal does not emerge as significant relative to the noise that accompanies the extratropical climate system.

Lin and Brunet (2009) found strong correlations between the height and SAT anomalies in eastern Canada

Fig. 5 For December–February at 42°N, 75°W, **a** above-average temperature anomalies and their associated MJO phases in the Wheeler-Hendon diagram of 8 MJO phases. The surface air temperature (SAT) data is band passed filtered between 20 and 100 days; **b** Same as **(a)** except for below-average SAT anomalies; **c** Percentage of above-average SAT anomalies in each MJO phase; **d** Percentage of below-average SAT anomalies in each MJO phase

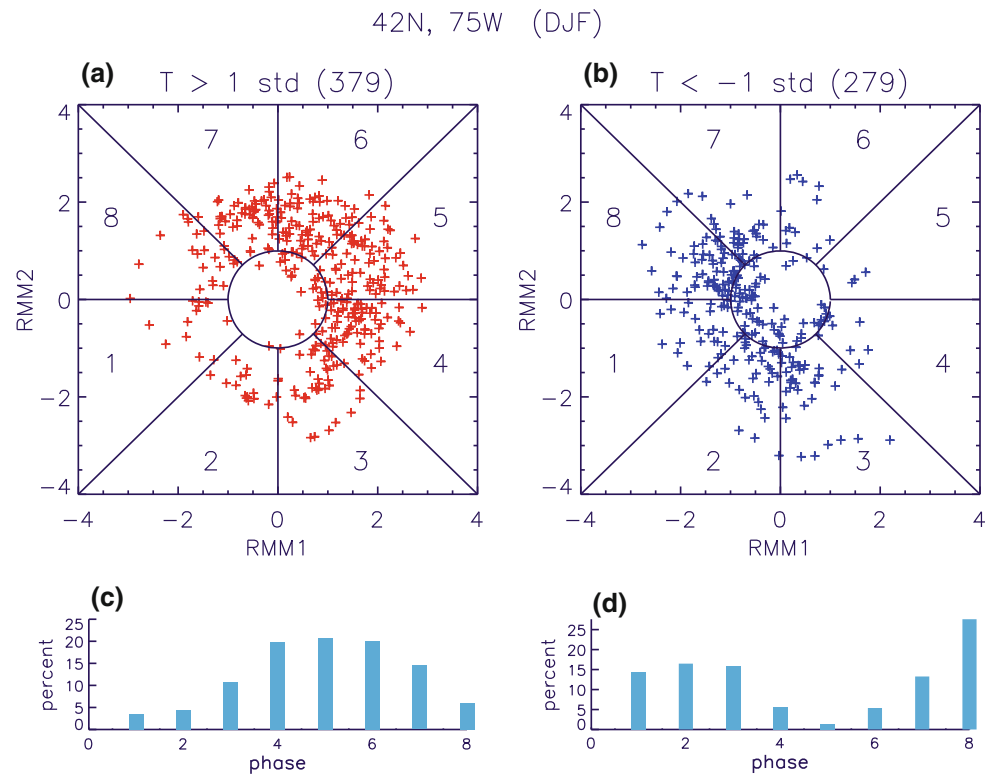
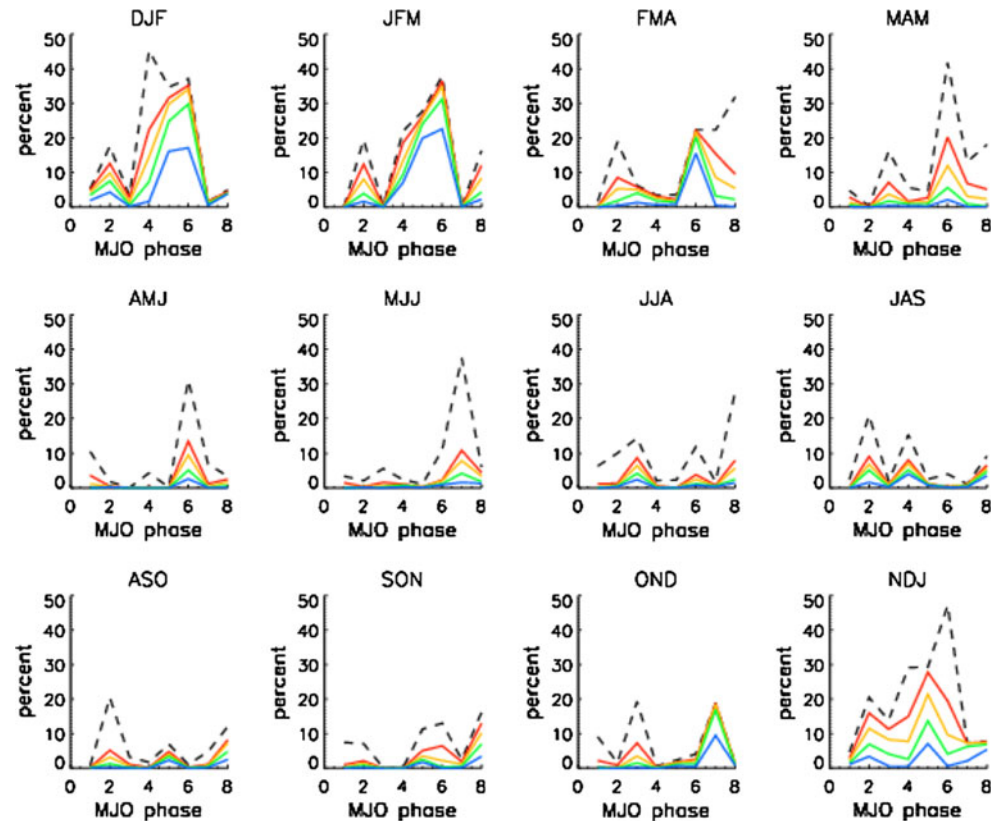


Fig. 6 For each overlapping 3-month season, the percent of area coverage of surface air temperature anomalies that have a confidence level of at least 95% and have different intraseasonal match levels. The x-axis indicates the 8 MJO phases. The intraseasonal match levels are 0% (dashed), 60% (red), 65% (orange), 70% (green) and 75% (blue), respectively



during the northern winter. They showed that the wave patterns over North America at 500-hPa are linked to wave trains emanating from an enhanced convective region in

the tropics. In Fig. 7, we show the MJO composites of 500-hPa geopotential height anomalies for DJF and JJA. The same 30 years of geopotential height data from the

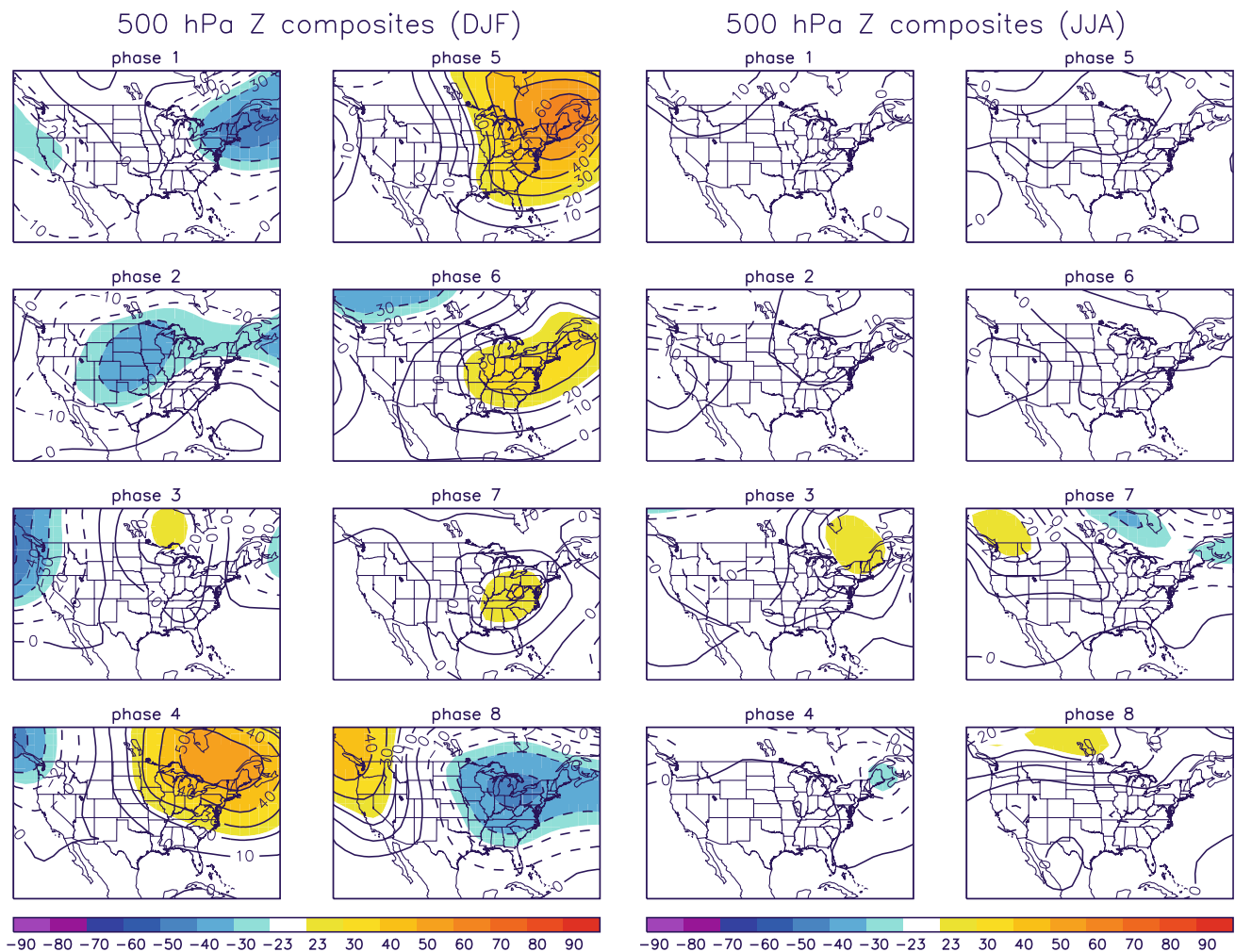


Fig. 7 Composites of 500-hPa geopotential height anomalies (in meters) as a function of the 8 MJO phases. The *white* area indicates a confidence level less than 95%. *Left* is for northern winter season (DJF) and *right* is for northern summer season (JJA)

NCEP-DOE Reanalysis-2 (Kanamitsu et al. 2002) are used to calculate composite anomalies, and similar Monte-Carlo procedures are used to determine statistically significant levels. In northern winter season (DJF) large positive anomalies are found in MJO phases 4, 5 and 6 over eastern US and Canada, while negative anomalies are found in MJO phases 8, 1 and 2 across the northeastern US. The height anomalies appear to have strong positive correlations with the SAT anomalies shown in Figs. 3 and 4. In the northern summer season (JJA) the height anomaly is generally small and not significant over the CONUS.

5 Composites of precipitation

Using the methodology similar to the composites of SAT, we construct MJO composites of precipitation anomalies over a larger region in North America including CONUS and Mexico. The results for twelve overlapping 3-month seasons

can be found on the NOAA CPC website (<http://www.cpc.ncep.noaa.gov/products/precip/CWlink/MJO/Composites/Precipitation/>). Figure 8 shows the percentages of area for precipitation composites which are statistically significant and include an intraseasonal match. In general, the area with significant precipitation anomalies is smaller than that for SAT anomalies.

During northern winter, the regions with a strong MJO signal in the precipitation composites differ from those in the SAT composites. Figure 9 shows precipitation composites for DJF season, which indicates above-average precipitation anomalies in the central plains of the US in MJO phases 4, 5 and 6. The anomalies are located to the west of an anomalous 500-hPa ridge (Fig. 7), indicating anomalous southerly flow and enhanced water vapor transport from the Gulf of Mexico.

In addition, MJO phase 3 is associated with a positive precipitation anomaly over the US west coast, including the states of California and Oregon (Fig. 9). These anomalies

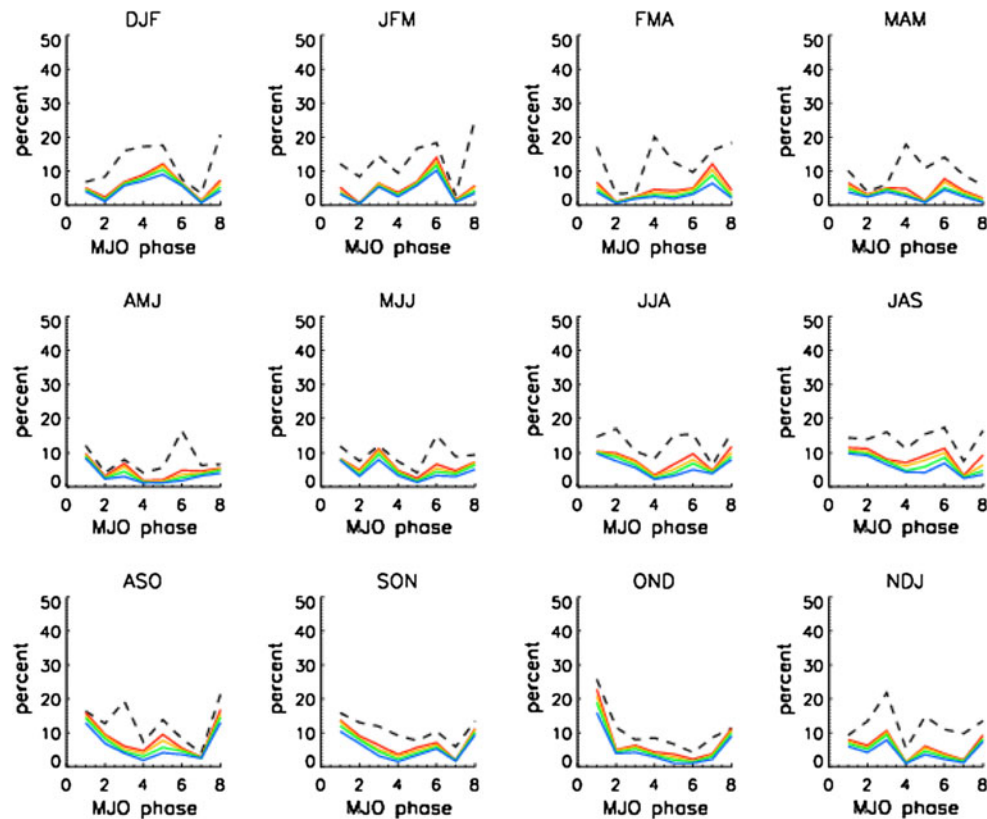


Fig. 8 Same as Fig. 6 except for US-Mexico precipitation anomalies

also exist for other winter season composites, such as OND and NDJ (not shown). This feature is in agreement with previous studies (e.g., Jones 2000), which showed that extreme precipitation events in California occur when enhanced convection is located over the Indian Ocean in association with strong MJO events.

Precipitation anomalies depend not only on water vapor transport, but also on the large-scale circulation. The latter includes divergent or convergent flow, as well as vertical motion. Figure 10 shows the MJO composites of vertical velocity anomalies at 500-hPa during DJF, which is calculated from the NCEP-DOE Reanalysis-2 data. Enhanced upward motion appears over regions of increased precipitation, such as the central plains of the US in MJO phase 5 and the west coast in MJO phase 3.

The MJO also affects subtropical precipitation in the northern summer and fall seasons. Figure 11 shows the precipitation composites for the July–September (JAS) season, when wet conditions are seen in eastern Mexico during MJO phase 1 and change to dry conditions in MJO phase 5. Maloney and Hartmann (2000b) found that when MJO wind anomalies in the lower troposphere of the eastern Pacific are westerly (i.e. MJO phase 1), Gulf of Mexico and western Caribbean hurricane genesis is four times more likely than when the MJO winds are easterly (i.e. MJO phase 5). Since JAS encompasses the peak of the

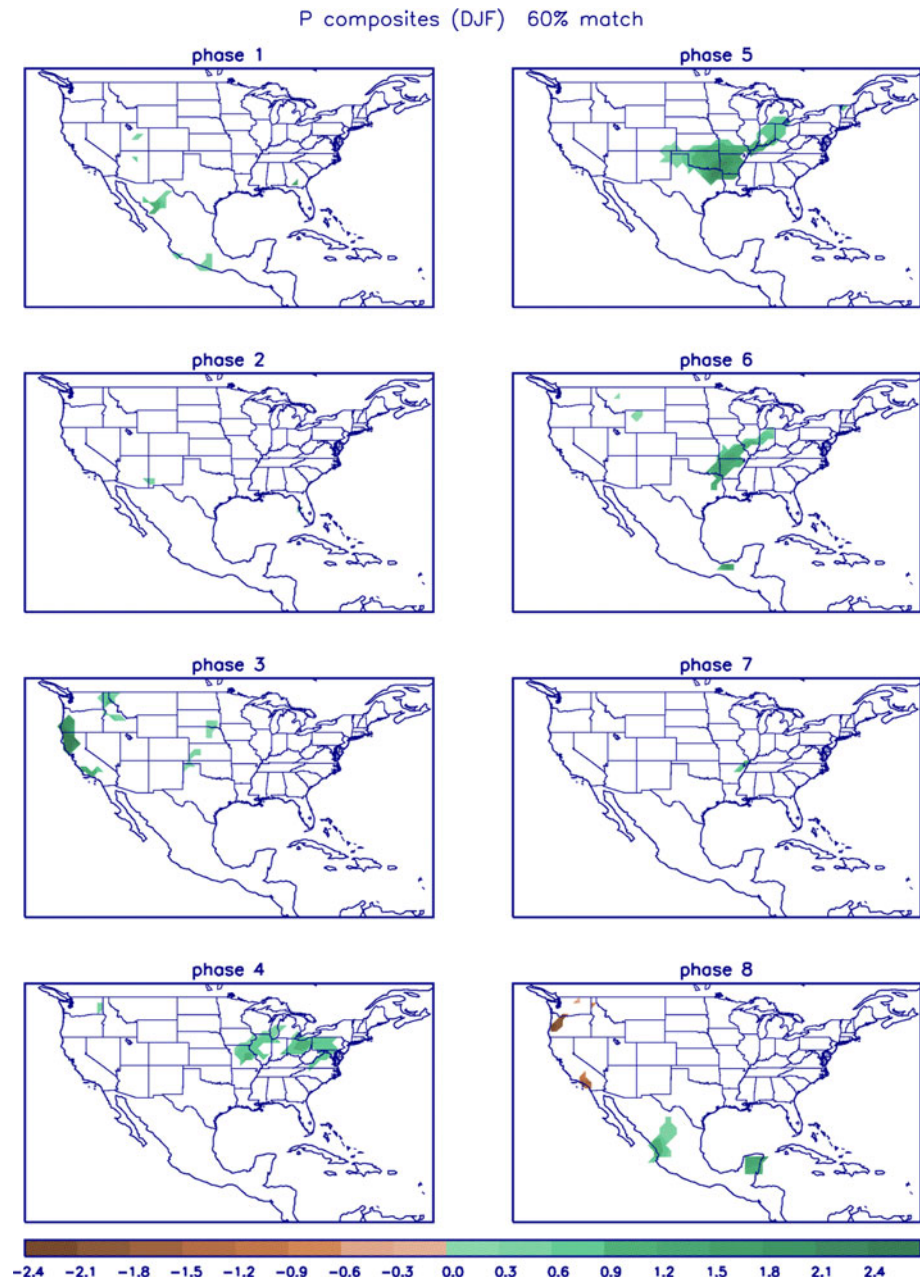
hurricane season over the eastern Pacific and western Atlantic, the precipitation anomaly in Mexico may reflect the MJO modulation of hurricane activity in the region. The JAS composites of 500-hPa vertical velocity anomaly also show good correspondence between vertical velocity and precipitation in eastern Mexico (not shown).

6 Potential predictability associated with the MJO composites

In the context of extended-range forecasting, the MJO composites discussed above can be used to specify SAT and precipitation anomalies if the future state of the MJO is known. There have been many studies on prediction of the MJO index, which are based on either complex climate models or statistical methods (Jones et al. 2000; Waliser et al. 2003; Lo and Hendon 2000; Jiang et al. 2008; Gottschalck et al. 2010). Those models and methods have achieved considerable skill at lead times up to 2–3 weeks.

To demonstrate the feasibility of using the MJO composites in SAT and precipitation forecasts, we compute the potential predictability from the use of MJO composites assuming that the future value of MJO phase is perfectly known. We make a three-category outlook: above normal (A), normal (N) and below normal (B) (Note that this is

Fig. 9 Same as Fig. 4 except for precipitation anomalies (mm/day) across the United States and Mexico. The daily precipitation data are smoothed by a 5-day running average

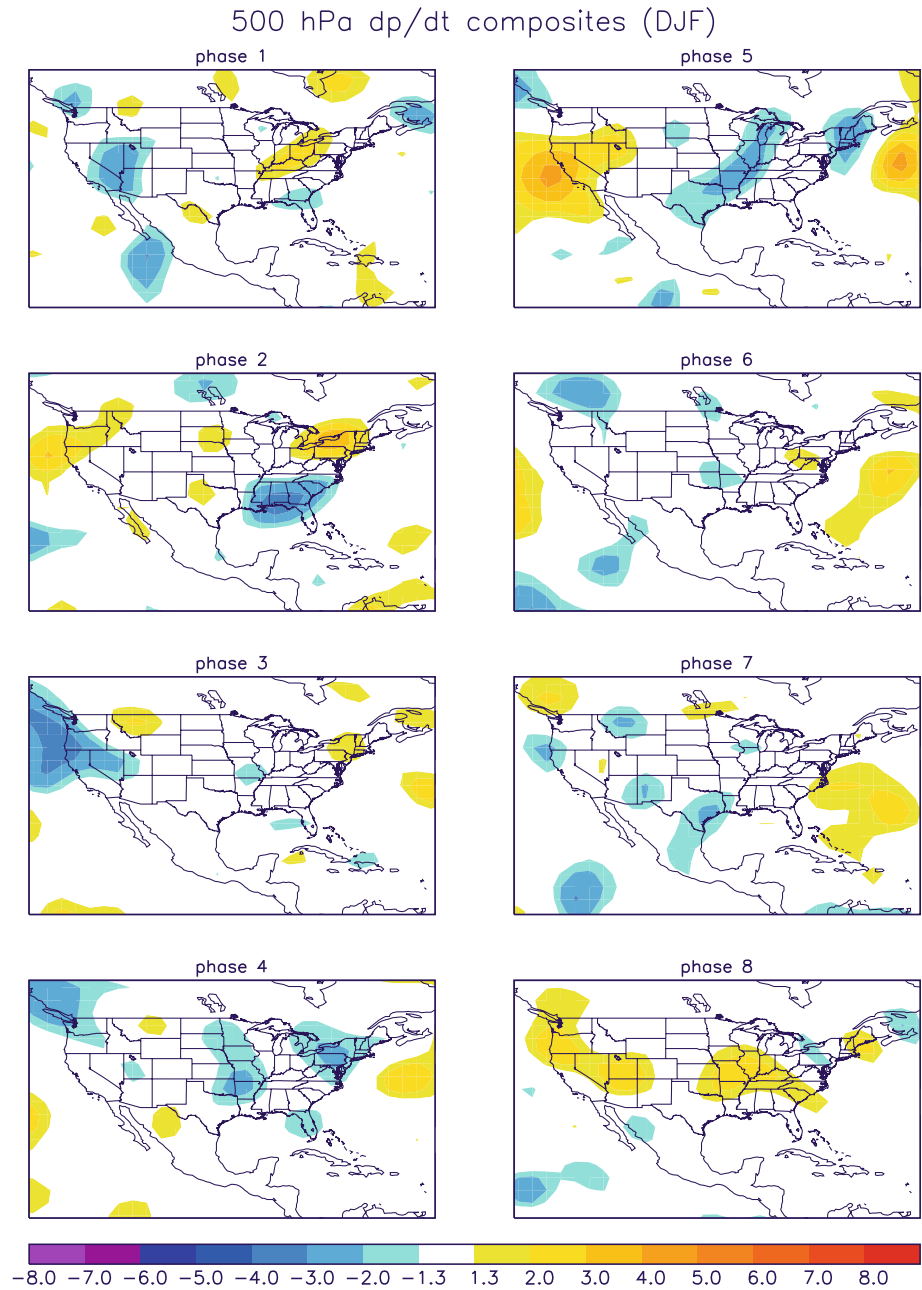


different from previous definition of “above average” and “below average” in Sect. 3). We make forecasts based on the composite for the central month of a season (January) using the seasonal (DJF) composites. Skill estimation follows the cross-validation with 1 year removed, i.e., we make a forecast for the target year using composites of the remaining 29 years. The forecast is only made over the regions with 95% statistical significance and varying levels of intraseasonal matching (four levels from 60 to 75%). We assume that prediction is for the above (below) normal category if the composite is positive (negative), regardless of the amplitude of the composite anomaly. We then compare the forecast fields with the observed fields to

determine the “hit” and “miss” rates, and calculate the Heidke skill scores (HSS) only over the regions where forecast is made.

Figure 12 shows the average HSS for 30 January forecasts of SAT and precipitation. In this example HSS is defined as: $HSS = (H - 1/3) / (1 - 1/3)$, where H is “hit” rate. Note that the “hit” rate is an average of forecast area only, which is a fraction of total composite area. No forecast is made in areas without a significant MJO effect. The percentage of the forecast area is also shown in Fig. 12 (shaded bars). Not all eight MJO phases are shown because in some MJO phases the composites have very little or no significant MJO effect, such as phases 3 and 7 in the SAT

Fig. 10 Composites of December–February 500-hPa pressure vertical velocity anomalies (Pa/s). Negative (*blue shading*) values indicate upward motion. The *white* area indicates less than 95% confidence

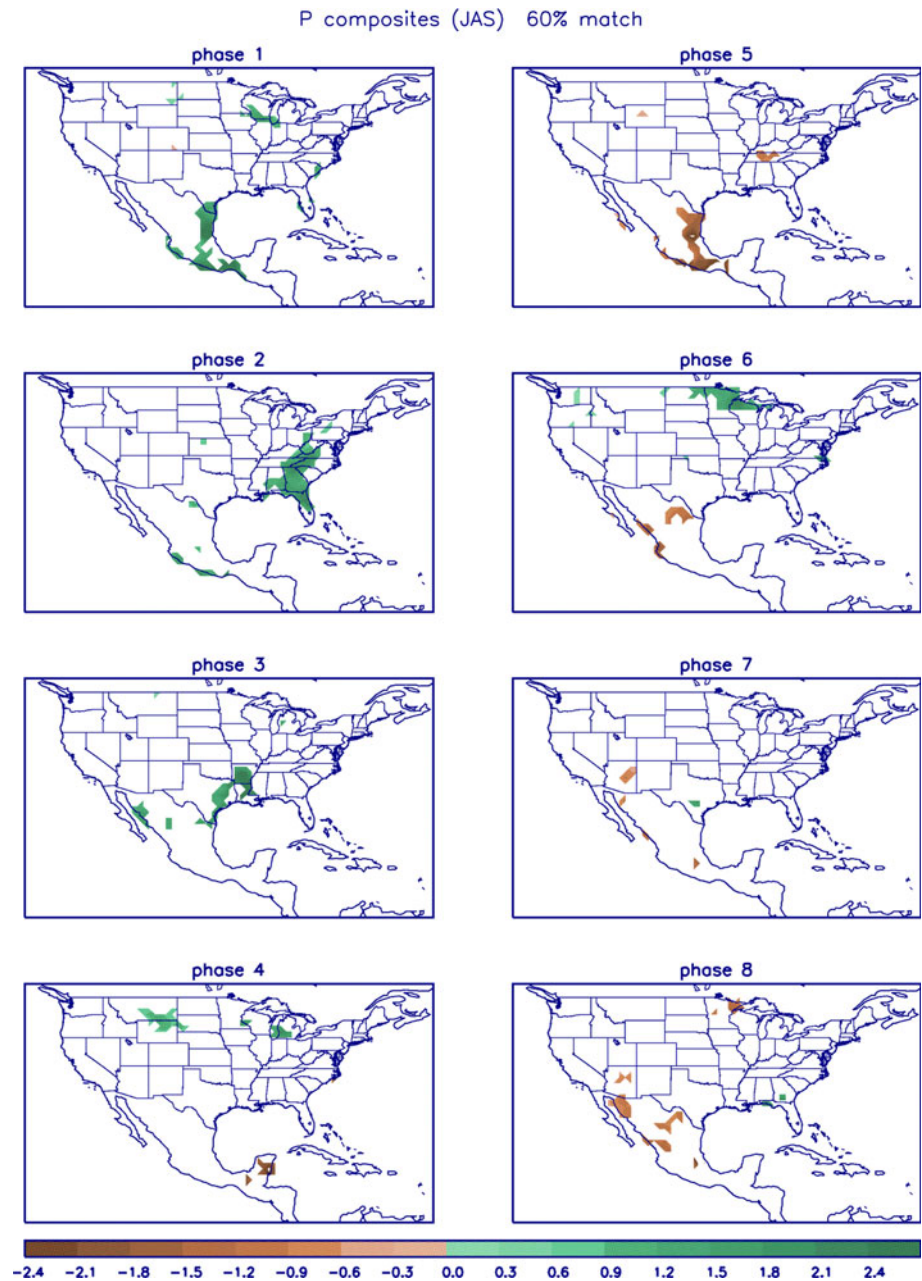


composites and phases 2 and 7 in the precipitation composites (Figs. 6 and 8). All the forecasts have a positive HSS, indicating potential skill using the MJO composites in an extended range (6–10 day and 8–14 day) outlook. As generally is the case with all climate forecasts, the skill for SAT is higher than that for precipitation. Also, it is evident that the intraseasonal match method does not necessarily lead to higher levels of skill in all MJO phases. It is possible that more skill could be realized by reducing the one standard deviation threshold or decreasing the 95% level of significance. However, this would come at the cost of ensuring the SAT anomalies are consistent with intraseasonal, MJO timescales.

7 Conclusions

This composite study of the MJO influence on the SAT and precipitation across the CONUS and Mexico complements previous composite studies of MJO impacts on the extratropics (e.g., Lin and Brunet 2009). The analysis provides a useful reference of when and where the MJO has significant impacts, and can be used as a prediction tool to complement the suite of extended range forecast tools used at the NOAA Climate Prediction Center. One defining attribute of this study is the option for “intraseasonal match,” which can be adjusted depending on the desired level of agreement between the raw SAT and precipitation

Fig. 11 Same as Fig. 9 except for the July–September season



anomalies and intraseasonal timescales. In general, the “intraseasonal match” technique shrinks the area that is significant using the Monte Carlo test, implying that the relatively lower frequency MJO signal in the middle latitudes is disrupted by higher frequency, synoptic-scale noise.

The composite results are compared to other studies, such as the MJO impact of extreme precipitation events in California and hurricane genesis in the Gulf of Mexico and western Caribbean (Jones 2000; Maloney and Hartmann 2000b). Although different approaches were used in those studies, the conclusions are consistent with those drawn from our composite analysis. In addition, the composites of

500-hPa height and vertical velocity anomalies are consistent with the composites of SAT and precipitation during the northern winter. It implies that the surface variability is largely influenced by the MJO modulated circulation over the extratropics. In other seasons, the MJO is generally not significant over the mid-latitudes, but remains evident in subtropical precipitation during the hurricane season.

It is demonstrated that there is potential forecast skill in the northern winter season, by using the MJO composites, provided that the dynamical or statistical tools can accurately predict the MJO phase. On the other hand, the MJO is of limited utility for North America outside of the northern winter because the influence of the MJO is

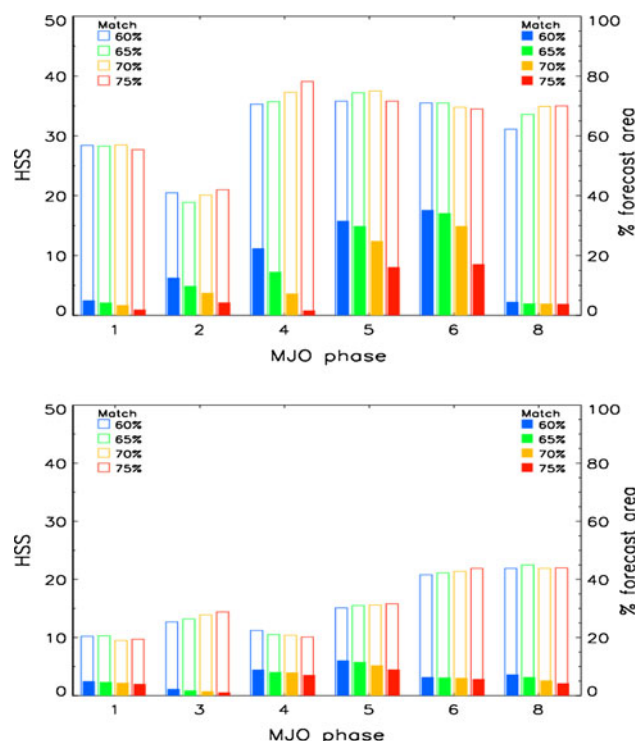


Fig. 12 The average Heidke skill score (HSS) for forecasts of January surface air temperature anomalies (*upper panel*) and precipitation anomalies (*lower panel*) as a function of the MJO phase and intraseasonal match level. The *shaded bars* indicate percentage of forecast area coverage. The forecasts are made by using December–February composites (using 29 years of data that does not include the forecasted year)

restricted to certain regions. An improved understanding of mechanisms linking the global tropics to the extratropical circulation patterns is critical to developing a better understanding the forecast potential of the MJO.

Acknowledgments We thank Jon Gottschalck, Peitao Peng, and Joseph Harrison of the NOAA Climate Prediction Center for helpful discussions, suggestions and assistance. We also thank two anonymous reviewers for their constructive comments and suggestions.

References

- Bond NA, Veehi GA (2003) The influence of the Madden-Julian Oscillation (MJO) on precipitation in Oregon and Washington. *Weather Forecast* 18:600–613
- Chang CP, Lim H (1988) Kelvin wave-CISK: A possible mechanism for the 20–50 day oscillation. *J Atmos Sci* 45:1709–1720
- Donald A, Meinke H, Power B, deMaia AHN, Wheeler MC, White N, Stone RC, Ribbe J (2006) Near-global impact of the Madden-Julian Oscillation on rainfall. *Geophys Res Lett* 33:L09704. doi: [10.1029/2005GL025155](https://doi.org/10.1029/2005GL025155)
- Gottschalck J, Wheeler M, Weickmann K, Vitart F, Savage N, Lin H, Hendon H, Waliser D, Sperber K, Prestrelo C, Nakagawa M, Flatau M, Higgins W (2010) A framework for assessing operational model MJO forecasts: a project of the CLIVAR

- Madden-Julian oscillation working group. *Bull Amer Meteor Soc* 91:1247–1258
- Hall JD, Matthews AJ, Karoly DJ (2001) The modulation of tropical cyclone activity in the Australian region by the Madden-Julian Oscillation. *Mon Weather Rev* 129:2970–2982
- Hendon HH, Liebmann B (1990) A composite study of onset of the Australian summer monsoon. *J Atmos Sci* 47:2227–2239
- Higgins RW, Mo KC (1997) Persistent North Pacific circulation anomalies and the tropical intraseasonal oscillation. *J Clim* 10:224–244
- Higgins RW, Shi W, Yarosh E, Joyce R (2000) Improved United States precipitation quality control system and analysis. NCEP/Climate Prediction Center Atlas No. 7, 40 pp
- Janowiak J, Bell G, Chelliah M (1999) A gridded data base of daily temperature maxima and minima for the conterminous US 1948–1993. NCEP/Climate Prediction Center Atlas, No. 6, CPC, NCEP, Camp Springs
- Jiang X, Waliser DE, Wheeler MC, Jones C, Lee M-I, Schubert SD (2008) Assessing the skill of an all-season statistical forecast model for the Madden-Julian oscillation. *Mon Weather Rev* 136:1940–1956
- Jin F-F, Hoskins BJ (1995) The direct response to tropical heating in baroclinic atmosphere. *J Atmos Sci* 52:307–319
- Jones C (2000) Occurrence of extreme precipitation events in California and relationships with the Madden-Julian oscillation. *J Clim* 13:3576–3587
- Jones C, Waliser DE, Schemm J-KE, Lau WKM (2000) Prediction skill of the Madden and Julian Oscillation in dynamical extended range forecasts. *Clim dyns* 16:273–289
- Kanamitsu M, Ebisuzaki W, Woollen JS, Yang S-K, Hnilo JJ, Fiorino M, Potter GL (2002) NCEP–DOE AMIP II reanalysis (R-2). *Bull Am Meteor Soc* 83:1631–1643
- Klotzbach PJ (2010) On the Madden-Julian Oscillation–Atlantic hurricane relationship. *J Clim* 23:282–293
- Knutson TR, Weickmann KM (1987) 30–60 day atmospheric oscillations: composite life cycles of convection and circulation anomalies. *Mon Wea Rev* 115:1407–1436
- L’Heureux ML, Higgins W (2008) Boreal winter links between the Madden-Julian Oscillation and the Arctic Oscillation. *J Clim* 21:3040–3050
- Lau K-M, Phillips TJ (1986) Coherent fluctuations of extratropical geopotential heights and tropical convection in intraseasonal time series. *J Atmos Sci* 43:1164–1181
- Lin H, Brunet G (2009) The Influence of the Madden-Julian oscillation on Canadian wintertime surface air temperature. *Mon Weather Rev* 137:2250–2262
- Lin H, Brunet G, Derome J (2009) An observed connection between the North Atlantic Oscillation and the Madden-Julian Oscillation. *J Clim* 22:364–380
- Lin H, Brunet G, Mo R (2010) Impact of the Madden-Julian Oscillation on wintertime precipitation in Canada. *Mon Weather Rev* 138:3822–3839
- Lo F, Hendon HH (2000) Empirical extended-range prediction of the Madden-Julian Oscillation. *Mon Weather Rev* 128:2528–2543
- Lorenz DJ, Hartmann DL (2006) The effect of the MJO on the North American monsoon. *J Clim* 19:333–343
- Madden RA, Julian PR (1994) Observations of the 40–50 day tropical oscillation—a review. *Mon Weather Rev* 122:814–837
- Maloney ED, Hartmann DL (2000a) Modulation of eastern North Pacific hurricanes by the Madden-Julian oscillation. *J Clim* 13:1451–1460
- Maloney ED, Hartmann DL (2000b) Modulation of hurricane activity in the Gulf of Mexico by the Madden-Julian Oscillation. *Science* 287:2002–2004
- Matthews AJ (2006) Propagation mechanisms for the Madden-Julian oscillation. *Q J Roy Meteor Soc* 126:2637–2651

- Mori M, Watanabe M (2008) The growth and triggering mechanisms of the PNA: a MJO-PNA coherence. *JMSJ* 86:213–236
- Murakami M (1979) Large-scale aspects of deep convective activity over the GATE data. *Mon Weather Rev* 107:994–1013
- Pai DS, Bhate J, Sreejith OP, Hatwar HR (2009) Impact of MJO on the intraseasonal variation of summer monsoon rainfall over India. *Clim Dyn*. doi:[10.1007/s00382-009-0634-4](https://doi.org/10.1007/s00382-009-0634-4)
- Straus DM, Lindzen RS (2000) Planetary-scale baroclinic instability and the MJO. *J Atmos Sci* 57:3609–3626
- Waliser DE, Lau KM, Stern W, Jones C (2003) Potential predictability of the Madden-Julian Oscillation. *Bull Am Meteorol Soc* 84:33–50
- Wheeler MC, Hendon HH (2004) An all-season real-time multivariate MJO index: Development of an index for monitoring and prediction. *Mon Weather Rev* 132:1917–1932
- Zhou S, Miller AJ (2005) The interaction of the Madden-Julian oscillation and the Arctic Oscillation. *J Clim* 18:143–159